that the remarkable chemical and physical properties of NO, which have only recently been linked to signaling between cells, appear to have long been exploited by fireflies to control signaling between individuals.

References and Notes

1. J. E. Lloyd, in *Sexual Selection and Reproductive Competition in Insects*, M. Blum, N. Blum, Eds. (Academic Press, New York, 1979), pp. 293–342.
2. M. A. Branham, M. D. Greenfield, *Nature* **381**, 745 (1996).
3. T. Wilson, J. W. Hastings, *Annu. Rev. Cell Dev. Biol.* **14**, 197 (1998).
4. T. A. Christensen, T. G. Sherman, R. E. McCaman, A. D. Carlson, *Neuroscience* **9**, 183 (1983).
5. H. Hashemzadeh, R. M. Hollingworth, A. Voliva, *Life Sci.* **37**, 433 (1985).
6. J. H. Buck, *Ann. N.Y. Acad. Sci.* **49**, 397 (1948).
7. H. Ghiradella, in *Insecta*, vol. 11A of *Microscopic Anatomy of Invertebrates*, F. W. Harrison, M. Locke, Eds. (Wiley-Liss, New York, 1998), pp. 363–381.
8. D. S. Smith, *J. Cell Biol.* **16**, 323 (1963).
9. J. F. Case, L. G. Strause, in *Bioluminescence in Action*, P. J. Herring, Ed. (Academic Press, New York, 1978), pp. 331–366.
10. *Photuris* fireflies used in this study have been identified by J. E. Lloyd (University of Florida, Gainesville) as belonging to a species group that cannot be distinguished with current taxonomic criteria: We refer to it here as *Photuris* sp.
11. *Photuris* sp. fireflies held for ~2.5 min in a mixture of N_2 and NO did not glow or flash until O_2 was reintroduced. This was not a "pseudoflash" response to O_2 deprivation as previously described by Buck (*6*), as O_2 reintroduction to insects maintained in pure N_2 for as long as 2 min did not evoke any bioluminescent response.
12. J. A. Wingrove, P. H. O'Farrell, *Cell* **98**, 105 (1999).
13. W. B. Grueber, J. W. Truman, *J. Comp. Neurol.* **404**, 127 (1999).
14. G. Bicker, *Trends Neurosci.* **21**, 349 (1998).
15. B. A. Trimmer *et al.*, data not shown.
16. Isolated, perfused lanterns were exposed to 0.5 mM of each NO donor diluted in saline from a stock solution of 100 mM in 1 mM NaOH. Light emission increased progressively throughout a 5-min application. Control application of saline containing only added NaOH had no effect on light production. cGMP levels were measured in lantern extracts with an enzyme immunoassay with samples from the nerve cord of the insect *Manduca sexta* used as a positive control. The lanterns contained about 10 fM cGMP per microgram of protein, and this was unaffected by prior treatment with the NO donor SNAP (1 mM).
17. D. M. Dawson, D. S. Bredt, M. Fotui, P. M. Hwang, S. H. Snyder, *Proc. Natl. Acad. Sci. U.S.A.* **88**, 7797 (1991).
18. R. M. Zayas, S. Qazi, D. B. Morton, B. A. Trimmer, *J. Comp. Neurol.* **419**, 422 (2000).
19. U. Muller, *Eur. J. Neurosci.* **6**, 1362 (1994).
20. S. M. Gibbs, J. W. Truman, *Neuron* **20**, 83 (1998).
21. E. Clementi, G. C. Brown, N. Foxwell, S. Moncada, *Proc. Natl. Acad. Sci. U.S.A.* **96**, 1559 (1999).
22. M. W. Cleeter, J. M. Cooper, V. M. Darley-Usmar, S. Moncada, A. H. Schapira, *FEBS Lett.* **345**, 50 (1994).
23. G. C. Brown, *Biochim. Biophys. Acta* **1411**, 351 (1999).
24. F. W. Cope, *Physiol. Chem. Phys.* **8**, 343 (1976).
25. J. Wood, J. Garthwaite, *Neuropharmacology* **33**, 1235 (1994).
26. V. Borutaite, A. Budriunaite, G. C. Brown, *Biochim. Biophys. Acta* **1459**, 405 (2000).
27. H. Achenbach, C. Walther, D. Wicher, *Neuroreport* **8**, 3737 (1997).
28. J. A. Nathanson, *Science* **203**, 65 (1979).
29. M. W. Vaughn, L. Kuo, J. C. Liao, *Am. J. Physiol.* **274**, H1705 (1998).
30. Supplementary material is available at www.sciencemag.org/cgi/content/full/292/5526/2486/DC1.
31. We thank J. Buck and J. Lloyd for inspiration, A. Gustafson and R. Willson for assistance with histochemistry and confocal microscopy, B. Michel and Z.

Femtomolar Sensitivity of Metalloregulatory Proteins Controlling Zinc Homeostasis

Caryn E. Outten[1] and Thomas V. O'Halloran[1,2]*

Intracellular zinc is thought to be available in a cytosolic pool of free or loosely bound Zn(II) ions in the micromolar to picomolar range. To test this, we determined the mechanism of zinc sensors that control metal uptake or export in *Escherichia coli* and calibrated their response against the thermodynamically defined free zinc concentration. Whereas the cellular zinc quota is millimolar, free Zn(II) concentrations that trigger transcription of zinc uptake or efflux machinery are femtomolar, or six orders of magnitude less than one atom per cell. This is not consistent with a cytosolic pool of free Zn(II) and suggests an extraordinary intracellular zinc-binding capacity. Thus, cells exert tight control over cytosolic metal concentrations, even for relatively low-toxicity metals such as zinc.

Zinc is an essential element for living organisms (*1*) and is the second most abundant transition metal in seawater and in humans. It is considerably less toxic than redox-active metals such as copper and is more soluble in oxygenated buffers than iron. Zinc serves as a cofactor in all six classes of enzymes as well as several classes of regulatory proteins (*2*, *3*). Several families of integral membrane proteins transport Zn(II), moving it across membranes into and out of cells (*4*, *5*). Less is known about the intracellular chemistry and mechanisms by which Zn(II) is sensed, stored, or incorporated as a cofactor. A common assumption is that Zn(II)-requiring enzymes and transcription factors passively acquire this essential cofactor from a cytosolic pool thought to be 10^{-5} to 10^{-12} M in free Zn(II) (*4*, *6–9*). Direct measurements of cytosolic zinc pools have proved difficult because fractionation can lead to cross contamination between intracellular sites.

Several Zn(II)-responsive transcription factors are known to mediate zinc homeostasis in vivo (*10–15*) and are thought to do so by monitoring changes in this hypothetical pool of free zinc. The mammalian MTF1 sensor is estimated to have a dissociation constant K_d below 90 μM (*4*). Estimates of the zinc sensitivity of the *Synechococcus* PCC7942 SmtB protein vary from <0.01 nM to 3.5 μM (*7*, *8*). Expression of *E. coli* zinc uptake and export genes is regulated by Zur and ZntR metalloregulatory proteins, respectively (*16–20*). We report here the mechanism of Zur and the calibration of both of these zinc-sensing metalloregulatory proteins to directly establish their functional "set point" relative to $[Zn(II)]_{free}$. The femtomolar sensitivity of the pair indicates that intracellular fluxes of zinc between metalloenzymes and metal sensor, storage, and transport proteins are likely to involve direct transfer of the ion between proteins in kinetically controlled substitution reactions.

The total zinc content of *E. coli*, also known as the zinc quota, was established by inductively coupled plasma mass spectrometry (ICP-MS) analysis of whole cell lysate. Cells accumulate each transition element to a different extent, but zinc is concentrated by the greatest factor (Fig. 1). Growth in a metal-depleted medium establishes the minimal quota for this element, or 2×10^5 atoms of zinc per cell [determined here as a colony-forming unit (CFU)] (*21*, *22*) (Fig. 1A). These quotas can be interpreted as total cellular concentrations by dividing the moles per cell by a maximum volume for a cell grown in this medium (Fig. 1, B and C). In the case of minimal medium, the minimal $[Zn(II)]_{total}$ corresponds to 0.2 mM. This value is ~2000 times the ambient total zinc concentration in this depleted medium (Fig. 1B). The ability of microbes to accumulate metals such as iron to such high concentrations under starvation conditions is well established, but not documented for zinc. Cells grown in a medium replete with metals accumulate twice as much zinc per cell; however, the cell volume also doubles (*23*, *24*), leaving the total zinc concentration unchanged (Fig. 1C). Thus, the total concentration of Zn(II) is

¹Department of Chemistry and ²Department of Biochemistry, Molecular Biology, and Cell Biology, Northwestern University, 2145 Sheridan Road, Evanston, IL 60208, USA.

*To whom correspondence should be addressed. E-mail: t-ohalloran@northwestern.edu

tightly controlled in bacteria cells. We note that the iron and calcium quotas measured for each *E. coli* cell are the same as that of zinc. This indicates similar cellular requirements for these metal ions under these growth conditions. Far lower requirements are observed for other essential metals such as manganese and copper.

To gauge how much of the total cellular zinc is free in the cytosol, we determined the in vitro zinc responses of Zur and ZntR under conditions in which the Zn(II) concentration can be precisely controlled (*25*). Zur binds DNA in the presence of Zn(II), and excess EDTA inhibits this binding (*17*); however, the molecular mechanism of transcriptional control has not been established. DNA footprinting (Fig. 2A) demonstrates that metal occupancy of Zur modulates

its DNA affinity; this directly controls the binding and activity of RNA polymerase (RNAP) at this promoter (*26*). The Zn_1Zur form was stable as isolated and did not bind DNA when contaminating Zn(II) in the buffer was sequestered by a stringent chelator (lane 2). In the absence of added Zn(II), Zur did not compete for DNA binding, allowing RNAP to bind (Fig. 2A, lane 5) and form an open complex. The addition of excess Zn(II) allowed Zur to bind to the *znuC* promoter (P_{znuC}), and this prevented RNAP binding (lanes 3 and 6). This presumably involves the Zn_2Zur form; however, the metal protein stoichiometry of the DNA binding form has yet to be established. The orientation of RNAP was determined by examining the location of deoxyribonuclease (DNase I) and $KMnO_4$ hy-

persensitive bands in the RNAP footprint (Fig. 2C). The DNase I hypersensitivities are usually found upstream of the transcription start site (−20 through −60 in Fig. 2A) (*19*). $KMnO_4$ hypersensitivity outlines the transcription bubble that extends from the −10 box to the transcription start site, establishing that RNAP forms an open complex poised to transcribe in the *znuC* direction of the promoter. The *znuC* promoter has an extended −10 (TGnTATTAT) with no clear −35 hexamer (Fig. 2C). Zur binding completely blocks the extended −10, thereby sterically hindering RNAP binding. These results directly establish a metal-induced repression mechanism for Zur.

Zur-DNA interaction correlated with the concentration of Zn(II) in the assay (Fig. 3). With *N,N,N′,N′*-tetrakis(2-pyridylmethyl)ethylenediamine (TPEN) present as a zinc buffer, the free zinc concentration at half-maximal Zur binding to the DNA is 9.6 (± 3.0) $\times 10^{-17}$ M. The $[Zn(II)]_{free}$ was calculated with $[TPEN]_{total}$, $[Zn(II)]_{total}$, and $K′$, the apparent binding constant at a given pH and ionic strength:

$$Zn(II)_{free} + TPEN \rightleftharpoons Zn\text{-}TPEN \qquad (1)$$

This value was calculated from the absolute binding constants for Zn-TPEN (*25, 27*). As shown in Eq. 2, log $K′_{Zn\text{-}TPEN} = 15.2$ at pH 7.6, 0.1 M ionic strength:

$$K′_{Zn\text{-}TPEN} = \frac{K_{Zn\text{-}TPEN}}{(1 + 10^{(pH - pK_{Zn})})(1 + 10^{(pK_{a1} - pH)})}$$

$$+ 10^{(pK_{a1} + pK_{a2} + pK_{a2} - 2pH)}$$

$$+ 10^{(pK_{a1} + pK_{a2} + pK_{a3} - 3pH)}$$

$$+ 10^{(pK_{a1} + pK_{a2} + pK_{a3} + pK_{a4} - 4pH)}$$

$$= \frac{10^{15.4}}{(1 + 10^{(7.6 - 9.11)})(1 + 10^{(7.23 - 7.6)})}$$

$$+ 10^{(7.23 + 4.92 - 15.2)}$$

$$+ 10^{(7.23 + 4.92 + 3.41 - 22.8)}$$

$$+ 10^{(7.23 + 4.92 + 3.41 - 2.99 - 30.4)})$$

$$= 1.71 \times 10^{15} \qquad (2)$$

where K_{a1}, K_{a2}, K_{a3}, and K_{a4} are successive protonation constants for TPEN.

To determine whether the zinc-dependent binding of Zur to DNA correlated with repression of the *znu* genes, we conducted in vitro run-off transcription assays with Zur and the *znu* Zn(II) uptake system (*28*). Amounts of *znuC* RNA transcript correlate with $[Zn(II)]_{free}$ (Fig. 4). With 25 μM TPEN in the buffer, half-maximal repression by Zur occurs when the total Zn(II) concentration is
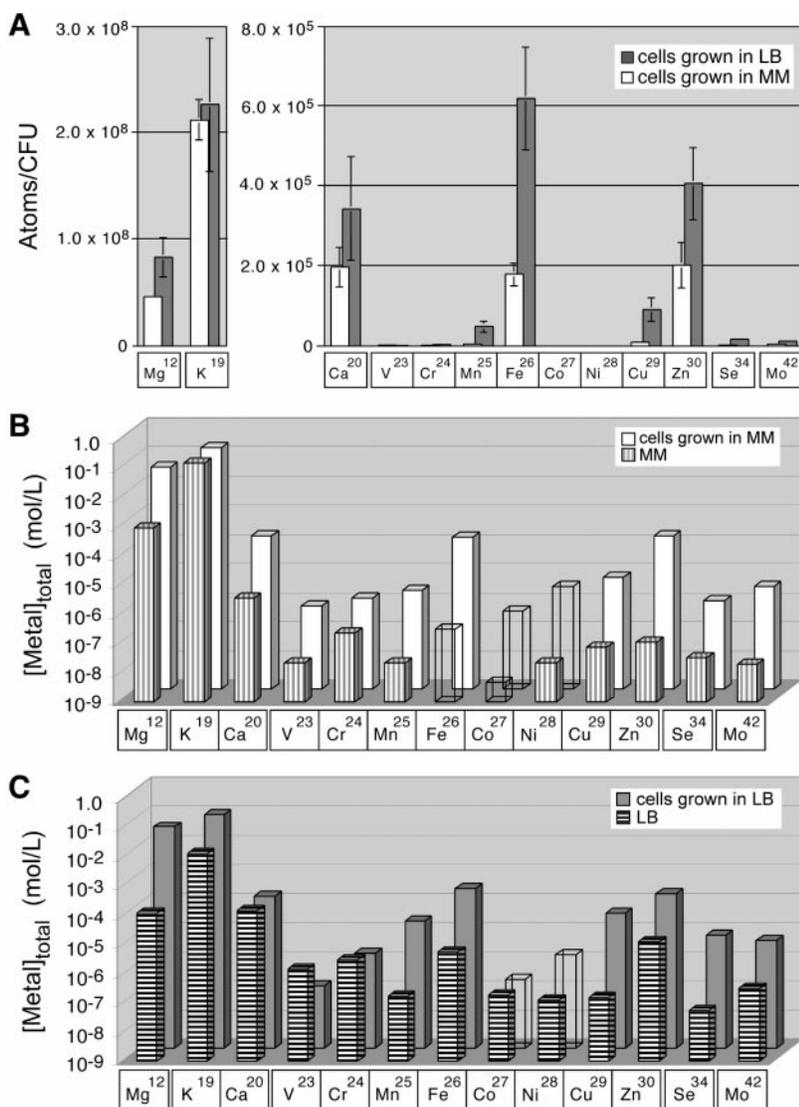

Fig. 1. Metal content of *E. coli* cells grown in LB and glucose minimal medium as determined by ICP-MS. (**A**) Atoms per cell (determined as CFU) for each metal ion in minimal (MM) and LB medium. The reported values are the mean of three independent measurements; error bars are SDs. (**B** and **C**) The *E. coli* metallome, i.e., the total metal content of the cell, is represented in terms of moles per cellular volume for cells grown in minimal medium (B) or LB medium (C) and compared with the total metal concentrations in the relevant growth medium (*22*). The unfilled columns represent detection limits for low-abundance elements under these experimental conditions.

Fig. 2. Zur footprinting and *znuC* promoter structure. (**A**) Zur DNase I (left, lanes 1 to 7), and KMnO$_4$ (right, lanes 1 to 6) footprinting with the nontemplate strand of P$_{znuC}$. Zur = 50 nM; RNAP = 50 nM; DNA = 1 nM; Zn(II) = 25 μM; TPEN = 10 μM. Lanes G are guanine-specific sequence ladders. (**B**) Mechanism for Zur regulation [extended (ext) −10]. The promoter location and protein-binding sites are scaled to match the gels shown in (A). (**C**) Summary of footprinting results from (A) outlining the Zur- and RNAP-binding sites and the *znuC* promoter structure. The extended −10 is outlined in black and the areas protected by Zur or RNAP from DNase I cleavage are highlighted in gray. Vertical arrows (↑ ↓) indicate DNase I–hypersensitive sites and asterisks (*) indicate KMnO$_4$-hypersensitive sites.

The transcription start site for the *znuC* RNA transcript (+1) was determined by primer extension (*39*). Dashed horizontal arrows indicate the location of the imperfect palindrome (*17*).
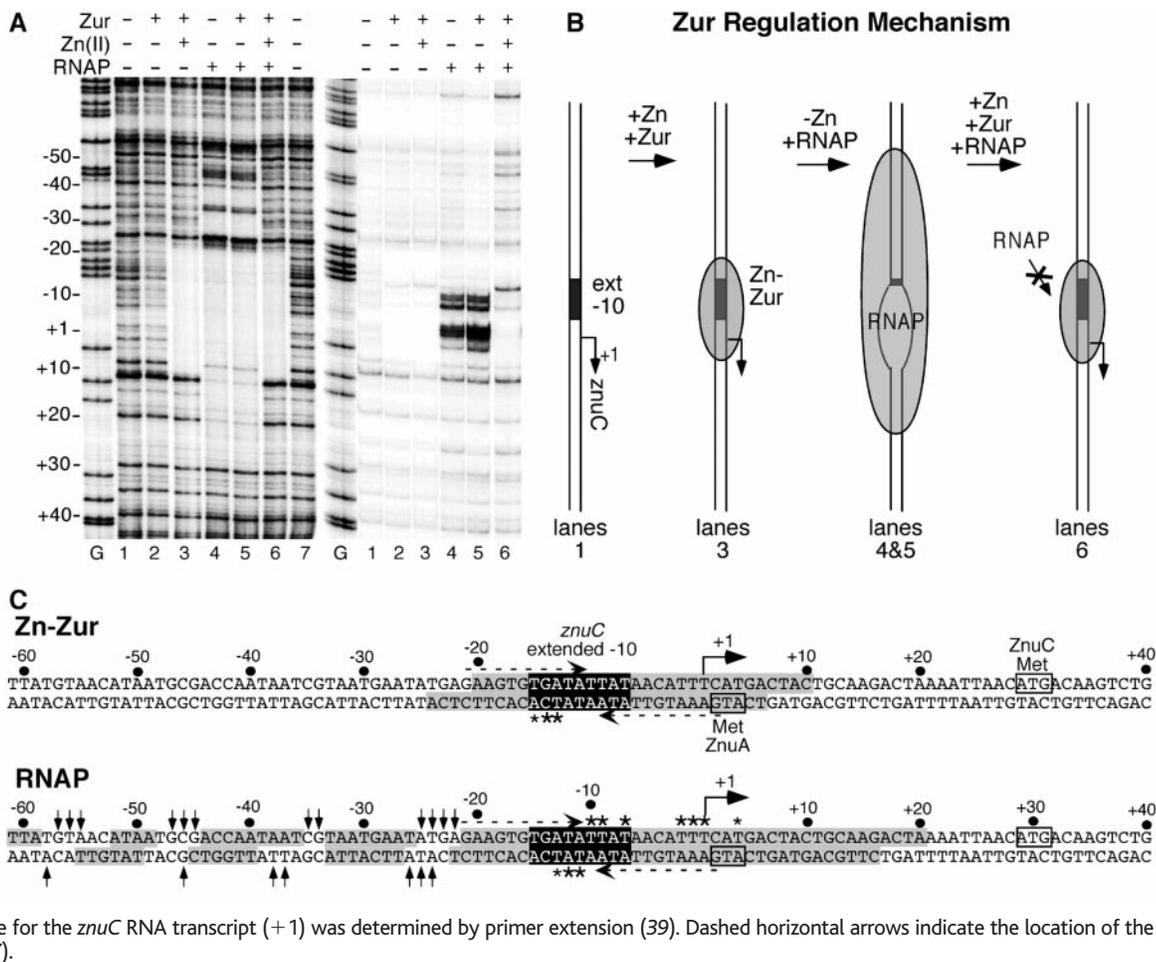
Fig. 3. DNase I footprinting of Zur and the template strand of P$_{znuC}$ with varying [Zn(II)]. Zur = 50 nM; DNA = 1 nM; Zn(II) = 0 to 30 μM; TPEN = 27.5 μM; [Zn(II)]$_{free}$ was calculated with [Zn(II)]$_{total}$, [TPEN]$_{total}$, and K′$_{Zn-TPEN}$. A mixture of Zur and a 340-bp DNA fragment containing the Zur operator was titrated with ZnSO$_4$ to a final concentration of 30 μM total Zn(II). The extent of projection of the footprinted region [see (*19*) for methods] in the left panel is plotted against [Zn(II)] free in the right panel.
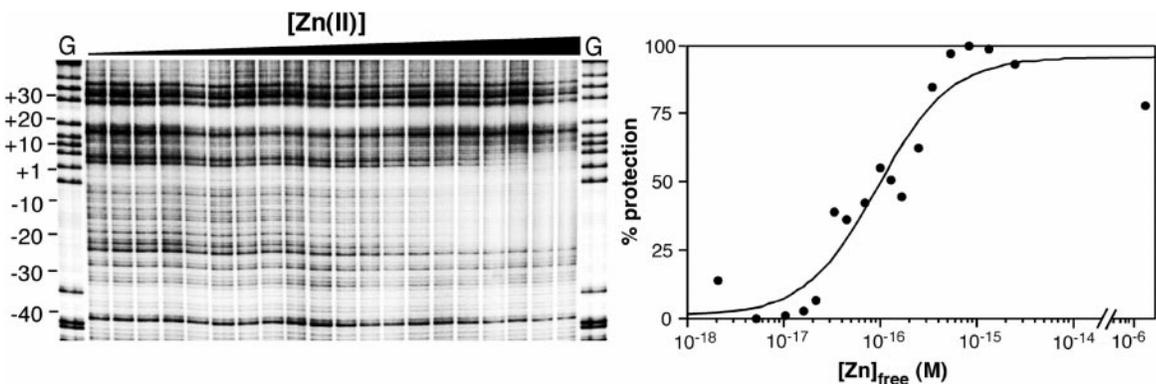

6.4 (±0.4) μM, which corresponds to [Zn(II)]$_{free}$ = 2.0 (±0.1) × 10^{-16} M. This value is very close to the [Zn(II)]$_{free}$ value from the independent Zur–DNA-binding assay, indicating that RNAP does not substantially affect the metal response of this Zn(II) receptor. Zur competes with TPEN for Zn(II), denoting a high Zn(II) affinity of this metalloprotein.

To establish the relative sensitivity of ZntR for Zn(II), we also conducted transcription experiments under identical conditions with ZntR and the *zntA* promoter (Fig. 4). Half-maximal activation by ZntR occurred at 16.6 (±0.7) μM Zn(II) with 25 μM TPEN, which corresponds to [Zn]$_{free}$ = 11.5 (±1.3) × 10^{-16} M. Independent measurements of ZntR affinity for Zn(II) reveal a similar value for the zinc-protein dissociation constant (*29*).

The transcriptional response profiles of the Zur-P$_{znuC}$ and ZntR-P$_{zntA}$ systems reveal that these proteins work in series to control zinc homeostasis. The precise zinc concentrations at which these systems switch on and off define the physiological onset of zinc starvation and zinc toxicity. As the cell acquires sufficient zinc for growth and cell division, expression of the *znu* uptake system is decreased. Once the minimal quota is slightly exceeded and the zinc burden of the cell begins to increase, the *zntA* efflux system is expressed. Comparison of the profiles provides a gauge of the optimal free zinc concentrations in the cells. The narrowness of this window reveals the delicate balance between Zn(II) deficiency and overload, suggesting a remarkably small tolerance range for cytoplasmic zinc.

Fig. 4. Zur and ZntR transcription assay results as a function of $[\text{Zn}]_{\text{free}}$. $[\text{RNAP}] = [\text{Zur}] = [\text{ZntR}] = 50$ nM, [DNA template] = 4 nM, [TPEN] = 25 μM. The dotted line and the solid line represent the fit of the Zur/P_{znuC} (open triangles) and ZntR/P_{zntA} (closed circles) data points, respectively, to a sigmoidal function. The area highlighted in gray is the range of $[\text{Zn}]_{\text{free}}$ between the half-maximal induction point on the two curves.
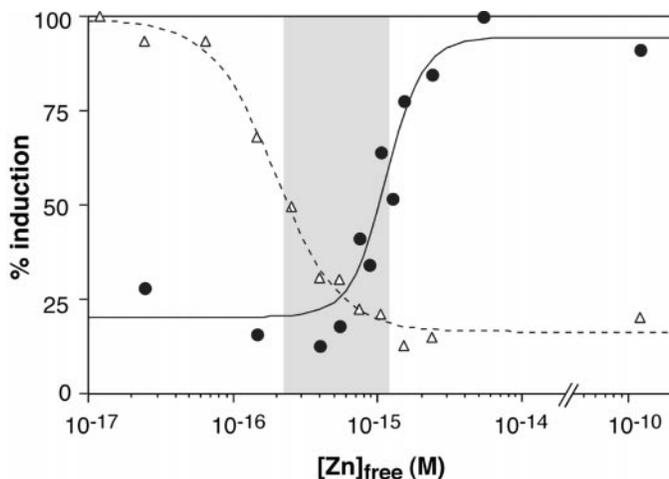
The magnitudes of these Zn(II) response thresholds are surprisingly small, especially when the volume of the cell is considered. In *E. coli,* cell volumes typically vary over a factor of 7 depending on the stage in the cell cycle or upon the nutrient content of the growth medium (*23, 24, 30, 31*). With 1.8×10^{-15} liter as the maximum volume of a typical *E. coli* cell in exponential phase in minimal growth medium, the lowest possible concentration of free zinc, corresponding to one zinc atom per cell, would be 1×10^{-9} M. Given that these key metalloregulatory proteins are saturated at a free zinc concentration of about 10^{-15} M, at least six orders of magnitude smaller than the absolute minimal value, we conclude that under normal growth conditions, there is no persistent pool of free Zn(II) ions in the cytoplasm. Initial reports for the SmtB metalloregulatory protein suggested a Zn(II) affinity in the 10^{-6} M range (*7*), but a more comprehensive study suggests a lower dissociation constant of $<10^{-11}$ M (*8*). The latter value is consistent with the proposal that free zinc in the cytosol is not physiologically available under standard growth conditions.

These results establish several key boundary conditions for the intracellular chemistry of zinc and suggest a reevaluation of its cell biology. Considering that zinc is accumulated to a total concentration of 0.2 mM, the term "trace element" is not a useful description of the zinc status from a cell's point of view. Extraordinary requirements for iron, an element not typically referred to as a trace substance in cells, are well established (*32*).

Despite the abundance of zinc in the cell, the extraordinary affinity of the primary zinc sensor/regulator proteins argues against a role for free Zn(II) ions in cytosolic cellular transactions. As first suggested for copper (*33*), the intracellular milieu apparently consists of a myriad of tight metal ion-binding sites, which greatly outnumber the full metal ion content of the cell. Comparison of the data in Fig. 1A with the limited *E. coli* proteome data available to date suggests a similar situation for Zn(II): At least 12% of the zinc quota (2×10^5 atoms per cell grown in minimal medium) is tied up by only eight proteins, the major known component being RNAP (5000 copies, two Zn per copy), and five tRNA synthetases (~2000 to 3000 copies each) (*24*). More than 40 additional *E. coli* proteins are known to require a tightly bound zinc; however, the copy numbers of these proteins are not known. A minimal estimate still accommodates the majority of atoms reported per cell in Fig. 1A. When one also considers the modest affinity of Zn(II) for nonspecific sites in the 10^6 proteins, 10^7 amino acids, and 10^8 nucleotide equivalents in DNA and RNA per cell, an overcapacity for binding of Zn(II) and other transition metals is not unreasonable. Mammalian cells in culture maintain a total zinc quota within a narrow range around 0.4 fmol per cell, corresponding to a total cellular Zn(II) concentration in the millimolar range (*4, 34*). It remains to be seen whether eukaryotic cells function without free zinc in the cytosol as well. Reports of high concentrations of free zinc in mammalian cells (*4, 6, 7, 9*) may reflect vesicular sites where free Zn(II) is maintained at high concentrations, as has been proposed elsewhere (*35*).

It is not clear how proteins that specifically require Zn(II) obtain this cofactor in the face of such an overcapacity for zinc sequestration; however, it appears unlikely that the cellular inorganic chemistry of zinc is under simple thermodynamic control. The most likely explanation may involve cytoplasmic zinc trafficking factors that control the kinetics of metal ion exchange between proteins, as has been proposed for the copper metallochaperone Atx1 (*36*).

References and Notes

1. B. L. Vallee, *Biofactors* **1**, 31 (1988).
2. J. E. Coleman, *Curr. Opin. Chem. Biol.* **2**, 222 (1998).
3. J. M. Berg, Y. Shi, *Science* **271**, 1081 (1996).
4. R. D. Palmiter, S. D. Findley, *EMBO J.* **14**, 639 (1995).
5. C. Rensing, M. Ghosh, B. P. Rosen, *J. Bacteriol.* **181**, 5891 (1999).
6. S. L. Sensi *et al.*, *J. Neurosci.* **17**, 9554 (1997).
7. S. R. Kar, A. C. Adams, J. Lebowitz, K. B. Taylor, L. M. Hall, *Biochemistry* **36**, 15343 (1997).
8. M. L. VanZile, N. J. Cosper, R. A. Scott, D. P. Giedroc, *Biochemistry* **39**, 11818 (2000).
9. R. J. P. Williams, J. J. R. Frausto da Silva, *Coord. Chem. Rev.* **200-202**, 247 (2000).
10. J. W. Huckle, A. P. Morby, J. S. Turner, N. J. Robinson, *Mol. Microbiol.* **7**, 177 (1993).
11. H. Zhao, D. J. Eide, *Mol. Cell. Biol.* **17**, 5044 (1997).
12. R. Heuchel *et al.*, *EMBO J.* **13**, 2870 (1994).
13. C. Thelwell, N. J. Robinson, J. S. Turner-Cavet, *Proc. Natl. Acad. Sci. U.S.A.* **95**, 10728 (1998).
14. V. K. Singh *et al.*, *Mol. Microbiol.* **33**, 200 (1999).
15. A. Gaballa, J. D. Helmann, *J. Bacteriol.* **180**, 5815 (1998).
16. S. I. Patzer, K. Hantke, *Mol. Microbiol.* **28**, 1199 (1998).
17. _____, *J. Biol. Chem.* **275**, 24321 (2000).
18. K. R. Brocklehurst *et al.*, *Mol. Microbiol.* **31**, 893 (1999).
19. C. E. Outten, F. W. Outten, T. V. O'Halloran, *J. Biol. Chem.* **274**, 37517 (1999).
20. M. R. Binet, R. K. Poole, *FEBS Lett.* **473**, 67 (2000).
21. *E. coli* strain BW25113 (*37*) was grown with shaking at 37°C in LB or Chelex-treated (Bio-Rad) A minimal medium (*38*) containing 0.2% glucose and 40 μg/ml of all 20 L-amino acids to an optical density at 600 nm of 0.5 to 0.6. The cells were harvested at midlog growth and washed three times with fresh media containing 1 mM EDTA and one time with Milli-Q water. The pelleted cells were dried overnight at 80°C in Teflon tubes, dissolved in concentrated nitric acid, and the metal content measured by ICP-MS (PQ ExCell, TJA Solutions, Franklin, MA). Parallel control experiments were run to determine the background metal contamination in the materials used. All glassware and plasticware was acid-washed before use.
22. The total cellular concentration of each element was calculated assuming a maximal cellular volume of 1.8 μm^3 for cells grown in minimal medium and 3.5 μm^3 in LB medium (*23, 31*). Metal concentrations in media were determined by inductively coupled plasma atomic emission spectroscopy (Thermo Jarrell Ash AtomScan 25 ICP-AES) for Mg, Ca, and K and ICP-MS for all other elements. Because transition metal concentrations in minimal medium were substantially lower than in LB, ICP-MS measurements of minimal media samples employed the standard addition method. This reduced matrix effects.
23. T. Akerlund, K. Nordstrom, R. Bernander, *J. Bacteriol.* **177**, 6791 (1995).
24. H. Bremer, P. P. Dennis, in *Escherichia coli and Salmonella: Cellular and Molecular Biology,* F. C. Neidhardt, Ed. (ASM Press, Washington, DC, 1996), vol. 2, pp. 1553–1569.
25. C. J. Fahrni, T. V. O'Halloran, *J. Am. Chem. Soc.* **121**, 11448 (1999).
26. Cloning and purification of Zur will be reported elsewhere (C. Outten, D. Tobin, J. Penner-Hahn, T. O'Halloran, in preparation). For DNase I footprinting, a 340-base pair (bp) fragment including the *znuACB* promoter was amplified by the polymerase chain reaction from *E. coli* DH5α, subcloned into pUC19 (New England Biolabs), and confirmed by DNA sequencing. Footprinting procedures were as described (*19*). The Zur protein, as isolated, contains two zinc atoms per monomer and is denoted Zn$_2$Zur. It was treated with 1 mM TPEN overnight, and concentrated in a 10-ml Amicon ultrafiltration cell to 500 μl, then diluted up to 10 ml in buffer without TPEN. This process was repeated two more times to remove any weakly bound zinc. This form of the protein contained 0.7 to 0.8 Zn atoms per Zur molecule as determined by ICP-AES and is denoted Zn$_1$Zur.
27. A. E. Martell, R. M. Smith, *NIST Critical Stability Constants of Metal Complexes* (NIST Standard Reference Database 46, v5.0, Plenum, New York, 1998).

2491

28. Run-off transcription procedures were as described (*19*). The *znu* transcription template was prepared in the same manner as the *zntA* template in (*19*) and digested with Bsp MI and Bbv I to make a 233-bp fragment. Different size templates were tested for Zur transcription assays and a transcript was always observed for *znuCB* but not *znuA*. Both promoters are active in vivo (*16, 17*). The *znuCB* promoter may be favored in in vitro transcription because it is stronger than the *znuA* promoter.

29. Y. Hitomi, C. E. Outten, T. V. O'Halloran, in preparation.

30. F. C. Neidhardt, J. L. Ingraham, M. Schaechter, *Physiology of the Bacterial Cell: A Molecular Approach* (Sinauer Associates, Sunderland, MA, 1990).

31. T. Ali Azam, A. Iwata, A. Nishimura, S. Ueda, A. Ishihama, *J. Bacteriol.* **181**, 6361 (1999).

32. J. Granger, N. M. Price, *Limnol. Oceanogr.* **44**, 541 (1999).

33. T. D. Rae, P. J. Schmidt, R. A. Pufahl, V. C. Culotta, T. V. O'Halloran, *Science* **284**, 805 (1999).

34. D. A. Suhy, K. D. Simon, D. I. Linzer, T. V. O'Halloran, *J. Biol. Chem.* **274**, 9183 (1999).

35. M. S. Nasir *et al.*, *J. Biol. Inorg. Chem.* **4**, 775 (1999).

36. D. L. Huffman, T. V. O'Halloran, *J. Biol. Chem.* **275**, 18611 (2000).

37. K. A. Datsenko, B. L. Wanner, *Proc. Natl. Acad. Sci. U.S.A.* **97**, 6640 (2000).

38. F. M. Ausubel *et al.*, Eds., *Current Protocols in Molecular Biology* (Wiley, New York, 1995), vol. 1.

39. F. W. Outten, unpublished data.

40. Supported by NIH training grant T32 GM08382 (C.E.O.) and NIH grants R01 GM38784 and DK52627 (T.V.O.). We thank F. W. Outten for *znuC* primer extension data, S. Shafaie for ICP-MS assistance, and Y. Hitomi, H. Godwin, and J. Widom for helpful discussions.

Contribution of Aerobic Photoheterotrophic Bacteria to the Carbon Cycle in the Ocean

Zbigniew S. Kolber,[1]* F. Gerald Plumley,[2] Andrew S. Lang,[3] J. Thomas Beatty,[3] Robert E. Blankenship,[4] Cindy L. VanDover,[5] Costantino Vetriani,[1] Michal Koblizek,[1] Christopher Rathgeber,[6] Paul G. Falkowski[1,7]

The vertical distribution of bacteriochlorophyll *a*, the numbers of infrared fluorescent cells, and the variable fluorescence signal at 880 nanometers wavelength, all indicate that photosynthetically competent anoxygenic phototrophic bacteria are abundant in the upper open ocean and comprise at least 11% of the total microbial community. These organisms are facultative photoheterotrophs, metabolizing organic carbon when available, but are capable of photosynthetic light utilization when organic carbon is scarce. They are globally distributed in the euphotic zone and represent a hitherto unrecognized component of the marine microbial community that appears to be critical to the cycling of both organic and inorganic carbon in the ocean.

Although closely related to purple photosynthetic bacteria, aerobic anoxygenic photoheterotrophs (AAPs) are obligate aerobes, with unusually high concentrations of carotenoids (*1–3*), low cellular contents of bacteriochlorophyll *a* (BChl*a*) (*4*), and while containing photosynthetic reaction centers (RC) and light harvesting complex I (LHI), they often lack LHII (*3*). Photosynthetic energy conversion has been confirmed in several species (*5–8*), but most known AAPs have been isolated from organic-rich environments (*9–11*), where they appear to be heterotrophic. Recently, AAPs were found throughout the surface waters of the oligotrophic ocean (*12*), however, their abundance, distribution, and potential ecological importance were unknown. Here, we report quantitative measurements of the vertical distribution of AAPs and BChl*a* in the open ocean, determine the photosynthetic competence of these organisms, and evaluate their contribution to the marine carbon cycle.

To characterize the vertical distributions of AAPs and their photosynthetic properties we used an Infrared Fast Repetition Rate (IRFRR) fluorescence transient technique (*12, 13*). Samples obtained from discrete depths were analyzed within 60 min of sampling (*14*). We assessed the distribution of AAPs using the BChl*a* fluorescence signal at 880 nm (Fig. 1A), and measured bulk BChl*a* by high-performance liquid chromatography (HPLC) (*15*) (Figs. 1A and 2A). The BChl*a* concentrations reached a maximum of 3 to 5 ng/liter at about 30 m and decreased to levels <0.01 ng/liter below 150 m (Fig. 1A). Chlorophyll *a* (Chl*a*), which in the open ocean is only found in oxygenic phytoplankton, was about 150-fold more abundant. The vertical distribution of Chl*a*, however, was closely correlated with BChl*a* (Fig. 1B). The HPLC-based estimates of BChl*a* corresponded to the in vivo fluorescence at 880 nm, allowing us to use the IRFRR signal (which reflects the radiative losses from LH antennae), to derive the concentration of BChl*a* in situ and vice versa.

To quantify the representation of AAPs, we counted the BChl*a*-containing and total, 4′6-diamidino-2-phenylindole (DAPI) stained cell numbers by epifluorescence microscopy (*16*) (Fig. 1C). Model II regression analysis of the relationship between the fluorescence signals, pigment concentrations, and cell counts reveals a significant correlation between the 880-nm fluorescence emission and BChl*a* ($r^2 = 0.68$, $F = 62.6$, Fig. 3A), and the IR fluorescent cell counts ($r^2 = 0.49$, $F = 21.6$, Fig. 3B). From these data, we calculated the average cellular BChl*a* content at 1.2×10^{-19} mol per cell. The morphology of a representative isolate from the surface waters (cylindrical motile cells, approximately 1.2 μm long, 0.7 μm in diameter) allows us to estimate the cell volume at about 0.5 μm³, a cell wet weight of 0.5 pg, and a cell dry weight of 0.05 pg, yielding a BChl*a*/dry weight ratio of about 2.4 μmol/g. This ratio is similar to that of *Erythrobacter longus* (*17*), but much higher than that of *Citromicrobium bathyomarinum* (*18*). Assuming 36 BChl*a* molecules/RC+LHI (*19*), we estimated about 2000 RCs per cell. The cellular BChl*a* content calculated here is about an order of magnitude lower than that of *Rhodobacter sphaeroides* (*20*), and the BChl*a*/RC ratio is also about fivefold less than that of typical purple nonsulfur bacteria (*19*). However, the effective photosynthetic absorption cross section measured at 470 nm (*12*) (about 62 Å²) was comparable to that measured in a laboratory culture of *R. sphaeroides* (about 70 Å²). By comparison, the effective absorption cross section in photosystem II reaction centers in phytoplankton averaged 420 Å², consistent with 200 to 300 Chl*a*/RCII. Although the rate of photon absorption/RC was sevenfold less than in their oxygenic planktonic counterparts, AAPs display a similar light utilization efficiency per unit of chromophore.

Fluorescence excitation spectra, recorded at the emission maximum of 875 nm (*21*)

[1]Environmental Biophysics and Molecular Ecology Program, Institute of Marine and Coastal Sciences, Rutgers University, 71 Dudley Road, New Brunswick, NJ 08901–8521, USA. [2]Institute of Marine Science, University of Alaska, Fairbanks, AK 99775, USA. [3]Department of Microbiology and Immunology, University of British Columbia, University Boulevard, Vancouver, BC, Canada V6T 1Z3. [4]Department of Chemistry and Biochemistry, Arizona State University, Tempe, AZ 85287–1604, USA. [5]Biology Department, College of William & Mary, Williamsburg, VA 23187, USA. [6]Department of Microbiology, University of Manitoba, 407 Buller Building, Winnipeg, MB, Canada R3T 2N2. [7]Department of Geology, Rutgers University, 610 Taylor Road, Piscataway, NJ 08854–8066, USA.

*To whom correspondence should be addressed. E-mail: zkolber@imcs.rutgers.edu